Control scheme including prediction and augmented reality for teleoperation of mobile robots

Emanuel Slawiñski* and Vicente Mut

Instituto de Automática (INAUT), Universidad Nacional de San Juan, Av. Libertador San Martín 1109 (oeste), J5400ARL San Juan, Argentina.

SUMMARY
This paper proposes a control scheme for the teleoperation of a mobile robot in presence of time delay. Our proposal uses a compensation of the time delay based on a human operator's model and a simple 3D augmented reality scheme; both are related through a prediction system. Unlike other strategies, the proposed scheme has a model of the human operator inside it, including his decision so that human and robot "push in the same direction." The stability of the teleoperation system adding the proposed control scheme is proven concluding how the time delay changes the convergence rate and the convergence ball size. Finally, to illustrate the performance and stability of the proposed control structure, several teleoperation experiments in presence of various delays are shown.

KEYWORDS: Augmented reality; Mobile robots; Prediction; Teleoperation; Time delay.

1. Introduction
Finding out how to link a controller and the man/woman is a key factor to reach high performance in tasks where the presence of them is necessary. One of such tasks is the robots teleoperation, which allows human operators to execute tasks in remote or hazardous environments.[14] In this work, bilateral teleoperation systems of mobile robots are analyzed. In these systems, the human operator drives a mobile robot moving in a remote environment. Today, there are many applications for robot teleoperation, including telemedicine, exploration, entertainment, tele-manufacturing, and many more.[11] However, the presence of time delay may induce instability or poor performance of a delayed system,[21,24,27] making the wide application of the teleoperation systems difficult.

Up to now, several control schemes for robots teleoperation have been proposed. Some of the main ones are: tele-programming[12,13] and supervisor control[6,26]; where the human operator supervises the task generating high-level commands. Such commands are sent to planning and control algorithms implemented on the remote robot, this method does not execute a continuous teleoperation. Another scheme is predictive display[4,16] where the remote robot is displayed to the human operator, who generates commands interacting

* Corresponding author. E-mail: slawinski@inaut.unsj.edu.ar

with the graphics environment. Here, an excellent model of the remote robot and environment should be available to achieve a good performance. A control scheme many times referenced in the teleoperation literature is the delay compensation based on transmitting the wave variables.[2,22] There are various strategies that modify such transmitted variables, as discussed in refs. [9, 19, 20, 36, 37]. In refs. [28, 30, 31], the delayed command generated by the human operator is compensated using a human operator's reaction model applied to the current state of the remote site and the delayed information perceived by him. In addition, there are several schemes for robots teleoperation based on different concepts,[14] for example, remote impedance control,[17,23] signal filtering,[35] predictive control,[25] control based on events,[11] control based on passivity considering the discrete system,[34] among others. The stability and performance of a teleoperation system are relevant aspects that should be analyzed.[3,18]

This paper proposes a control scheme for bilateral teleoperation of mobile robots in presence of time delay. Our proposal combines a compensation of the time delay based on a human operator's model, a prediction system, and a simple 3D augmented reality scheme. The prediction system includes a predictor with bounded output on the local site and a Kalman filter, with a variance that depends on the current fictitious force, on the remote site. The compensation of the time delay uses an estimated value of where the human operator wants to go, which is calculated by the proposed prediction system. In addition, the 3D augmented reality scheme uses an estimated value of where the mobile robot will go, which is computed by such prediction system, too. Thus, the compensation of the time delay and the 3D augmented reality scheme are indirectly linked through the prediction system.

Ultimately bounded stability of the proposed teleoperation system is proven and how the time delay changes the convergence rate and the convergence ball size is analyzed. In addition, the software implementation of the proposed scheme is described in this work. Finally, to illustrate the performance and stability of the proposed control scheme for bilateral teleoperation of mobile robots with time delay, several teleoperation experiments are shown.

The paper is organized as follows: Section 2 gives the notation used in this paper. In Section 3, some background material on the stability of delayed systems is introduced. Section 4 presents the statement of the control problem. In

Section 5, the model of the human operator is presented, where his decision is considered. In Section 6, the stability of the nondelayed teleoperation system is analyzed. In Section 7, a control scheme for bilateral teleoperation of mobile robots is proposed and the stability of the delayed teleoperation system is proven. Section 8 describes the software structure developed to implement the proposed scheme. In Section 9, the stability and performance of the proposed control scheme are analyzed, making use of experiments on robots teleoperation. Finally, the conclusions of this paper are given in Section 10.

2. Notation

In this paper, $h(t) \in \Re^+$ denotes the time delay. We assume that the delay is finite and $\dot{h}(t) < 1$. If $\mathbf{x} \in \Re^n$, then $|\mathbf{x}|$ and $|\mathbf{x}|_\infty$ are the Euclidean and infinite norm of $\mathbf{x}$, respectively. If $\mathbf{B}$ is a matrix or vector then $\mathbf{B}^T$ is the transpose of $\mathbf{B}$. On the other hand, x_t (for a given time instant t) is the function defined by $x_t(\theta) = \mathbf{x}(t + \theta)$ for $\theta \in [-h(t), 0]$, for example, $x_t(0) = \mathbf{x}(t)$, $x_t(-h) = \mathbf{x}(t - h)$, and the norm $\|.\|$ is defined by $\|x_t\| = \sup_{\theta \in [t-h(t),t]} |\mathbf{x}(\theta)|$. Here, C is the Banach space (using norm $\|.\|$) of continuous functions on the interval $[t - h(t), t]$ at any time t, and $C_H := \{\psi \in C: \|\psi\| \leq H\}$, where $H \in \Re^+$. The induced norm of a nonlinear differentiable function g_1 represented by $\dot{x}(t) = g_1(\mathbf{x}(t), \mathbf{x}(t - h))$ is defined as $|g_1| = \sup(|g_1(\mathbf{x}_1, \mathbf{x}_2) - g_1(\mathbf{y}_1, \mathbf{y}_2)|/|[\mathbf{x}_1 \ \mathbf{x}_2] - [\mathbf{y}_1 \ \mathbf{y}_2]|)$ with $\forall \mathbf{x}_1, \mathbf{x}_2, \mathbf{y}_1, \mathbf{y}_2 \in \Re^n / [\mathbf{x}_1 \ \mathbf{x}_2] - [\mathbf{y}_1 \ \mathbf{y}_2] \neq \mathbf{0}$.

3. Exponential stability for nonlinear systems with time-varying delay

Let us consider the delayed functional differential equation given by

$$\dot{x}(t) = f(t, x_t), \qquad (1)$$

where $\mathbf{x} \in \Re^n$, $x_t \in C$, t, $t_0 \in \Re^+$, and $f: \Re^+ \times C \to \Re^n$ with $f(t, 0) = \mathbf{0}, \forall t \geq t_0$. Here, f is continuous and converters bounded sets into bounded sets. We assume that there exists a solution $\mathbf{x}(t; t_0, \psi_0)$ of Eq. (1) which depends continuously on the initial data $[t_0, \psi_0]$, where $\psi_0 = \mathbf{x}(t_0 + \theta)$ for $\theta \in [-h(t_0), 0]$ with $\psi_0 \in C_H$. Sufficient conditions implying existence, uniqueness, and continuous dependence can be found in the standard theory, e.g. in refs. [7, 10]. From now onward, we will denote the solution norm by $|\mathbf{x}(t; t_0, \psi_0)| = |x_t(0)|$. The right-hand side of (1) is a function of t, and a functional of x_t, i.e. to any t and any function $\psi_t \in C$ corresponds a vector $f(t, \psi_t) \in \Re^n$.

Fact 1.[29] *The zero solution (that is $\psi_0 = \mathbf{x}(t_0 + \theta) = \mathbf{0}$ for $\theta \in [-h(t_0), 0]$) of the delayed system $\dot{\mathbf{x}} = f(t, x_t)$, where f is supposed to map bounded sets of C into bounded sets of $\Re^n$ and the time delay is bounded by $h_m = \sup_{t \geq t_0} h(t)$, is exponentially stable if there exists a differentiable functional $V: \Re^+ \times C \to \Re^+$, and the following conditions hold:*

$$a\,|x_t(0)|^p \leq V(t, x_t) \leq b\|x_t\|^p, \qquad (2)$$

$$\dot{V}(t, x_t) \leq -c|x_t(0)|^p, \qquad (3)$$

where a, b, c are positive constants, p is a positive integer, and $\dot{V}(t, x_t)$ is the time derivative of $V(t, x_t)$ along the system trajectories (1). The solution of the system has an upper bound defined by $|\mathbf{x}(t; t_0, \psi_0)| \leq a_2\|\psi_0\|e^{-b_2 t}, \forall t \geq t_0 \geq 0$, where $b_2 = c/bpd^p$, $a_2 = (b/a)^{1/p}$ and d is the solution of $d = e^{(c/bp)(1/d^p)h_m}$.

Now, let us consider a nonlinear system with time-varying delay described by

$$\dot{\mathbf{x}}(t) = f_1(\mathbf{x}(t)) + g_1(\mathbf{x}(t), \mathbf{x}(t - h)), \qquad (4)$$

where $\mathbf{x} \in \Re^n$, t, $t_0 \in \Re^+$, $f_1: \Re^n \to \Re^n$ and $g_1: \Re^n \times \Re^n \to \Re^n$, with $f_1(\mathbf{0}) = \mathbf{0}$ and $g_1(\mathbf{0}, \mathbf{0}) = \mathbf{0}$ $\forall t \geq t_0$. In addition, we assume that f_1 and g_1 map bounded sets ($\Re^n$ and $\Re^n \times \Re^n$, respectively) into bounded sets in $\Re^n$. The time delay h in this context is caused by the transmission of signals through a communication channel. It is modeled as in ref. [33], where $0 \leq h(t) \leq h_m$ and $\dot{h}(t) < \tau < 1$, with $h_m \in \Re^+$.

Fact 2.[29] *Let us suppose that the subsystem $\dot{\mathbf{x}} = f_1(\mathbf{x})$ of the system (4) is exponentially stable with rate λ, then the following condition ensures the exponential stability of the delayed system (4):*

$$-\lambda + |g_1|\left[\frac{2 - (3/2)\tau}{1 - \tau}\right] < 0, \qquad (5)$$

where $\lambda, |g_1|, h_m \in \Re^+$ and $\dot{h}(t) < \tau < 1$. The norm $|g_1|$ is the induced norm of the function $g_1(.)$.

Corollary 1. *The functional V used in Fact 2, given by $V = \frac{1}{2}\mathbf{x}^T\mathbf{x} + \frac{1/2|g_1|}{1-\tau}\int_{t-h}^t \mathbf{x}^T(\theta)\mathbf{x}(\theta)d\theta$, defines a bound for the real response of the delayed system with coefficients a_2 and b_2 (which are defined in Fact 1) calculated from Fact 2, whose proof establishes that $p = 2$, $a = 0.5$, $b = 0.5(1 + |g_1|h_m/(1 - \tau))$, $c = \lambda - |g_1|((2 - (3/2)\tau)/(1 - \tau))$, and $|\partial V/\partial \mathbf{x}| \leq |\mathbf{x}|$.*

Corollary 2. *From Fact 1, Corollary 1, and defining $A_1 = d^2 \ln d$ and $A_2 = \frac{h_m}{2}\frac{c}{b}$, $\frac{\Delta A_1}{\Delta(d^2)} > \frac{\Delta A_2}{\Delta(c/b)}$ if the solution for d of the equation $d = e^{(c/b)(1/d^2)(h_m/2)}$ is such that $1 + \ln d^2 > h_m/2$, where $\Delta A_1/\Delta(d^2)$ is the variation of A_1 with respect to a variation in d^2 and $\Delta A_2/\Delta(c/b)$ is the variation of A_2 with respect to a variation in c/b.*

Proof. From Fact 1, $d \geq 1$ is the solution of $d = e^{(c/bp)(1/d^p)h_m}$, which, considering logarithms properties and $p = 2$ from Corollary 1, can be rewritten as $A_1 = A_2$, where $A_1 = d^2 \ln d^2$ and $A_2 = (h_m/2)(c/b)$. The derivative of A_1 with respect to d^2 is $1 + \ln d^2$ and the derivative of A_2 with respect to c/b is $h_m/2$. Therefore, Corollary 2 is demonstrated by simple comparison between the calculated derivatives. $\square$

4. Statement of the Control Problem

This section describes the analyzed control problem on a bilateral teleoperation system of mobile robots (Fig. 1). The human operator drives a mobile robot using a steering wheel
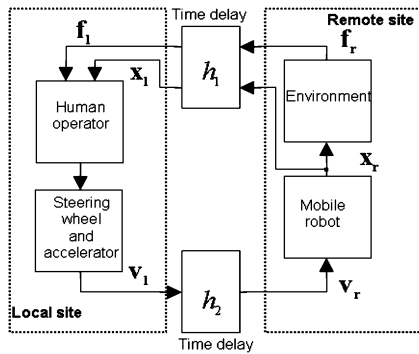
Fig. 1. General block diagram of a teleoperation system of a mobile robot.

and an accelerator pedal to generate velocity commands, which are sent to the remote site to be executed by the mobile robot. The mobile robot and the obstacles are visually back-fed to the human operator, which does not receive physical force feedback. We assume that the visual information of the obstacles position received by the human operator is not omitted by him. Then, such information can be interpreted as a fictitious force, which depends on the distance between the mobile robot and the obstacle.

The main signals of the system are the position $\mathbf{x_r}$ and fictitious force $\mathbf{f_r}$ on the remote site, the position $\mathbf{x_l}$ and fictitious force $\mathbf{f_l}$ on the local site, the velocity command $\mathbf{v_l}$ generated by the human operator, and the velocity reference $\mathbf{v_r}$ applied to the mobile robot.

On the other hand, the communication channel is represented by a time delay h defined as

$$h(t) = h_1(t) + h_2(t), \qquad (6)$$

where h_2 is the forward delay (from the local site to the remote site) and h_1 is the backward delay (from the remote site to the local site). We assume that $\dot{h} < \tau < 1$, where τ can be estimated for a real communication channel.[33]

We will consider the mobile robot located at a nonzero distance from the goal frame called ⟨goal⟩. In addition, attached to the robot there exists the frame called ⟨robot⟩. The vehicle position $\mathbf{x_r}$ is described in polar coordinates, where the state variables that define the mobile robot position are the distance error ρ and the angular error α. They are measured between the frame ⟨goal⟩ and the frame ⟨robot⟩ (Fig. 2).
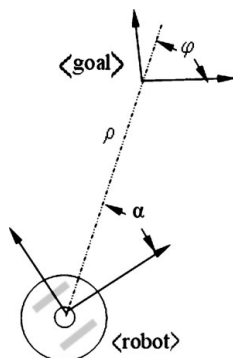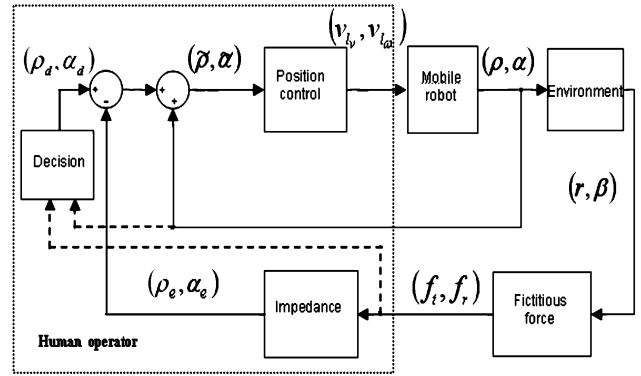

Fig. 2. Position and orientation of a mobile robot.

Fig. 3. Model of the human operator driving a mobile robot without time delay.

The kinematic equations, considering the fixed goal, can be written, not considering the final orientation φ in this case, as in ref. [1]

$$\begin{cases} \dot{\rho} = -v_{r_v} \cos\alpha \\ \dot{\alpha} = -v_{r_\omega} + v_{r_v} \dfrac{\sin\alpha}{\rho} \end{cases}, \qquad (7)$$

where v_{r_v} and v_{r_ω} are the linear and angular velocity of the mobile robot, respectively.

The objective of the teleoperation system is that a human operator drives a remote mobile robot to reach the goal frame ⟨goal⟩ in spite of the time-varying delay. The goal is described by $\mathbf{x_g} = [\mathbf{x_{g_x}} \ \mathbf{x_{g_y}}]$ where $\mathbf{x_{g_x}}$, $\mathbf{x_{g_y}}$ are the Cartesian coordinates in 2D.

5. Model of the Human Operator
The proposed model of a human operator is based on our previous papers[28,30–32] including a kinematic model and an impedance model to describe the position control and the reaction of the human operator in presence of obstacles, respectively. In this paper, we add a decision block, which generates an output signal from the mobile robot position and the fictitious force.

The proposed model of the human operator will be used later by the proposed control scheme for bilateral teleoperation of mobile robots. Figure 3 shows a block diagram describing a bilateral teleoperation system of a mobile robot without time delay including the model of the human operator, which will be described in the following subsections.

5.1. Proposed nonlinear kinematic model of the human operator
A nonlinear kinematic model to describe the position control executed by a human operator driving a mobile robot is proposed in refs. [28, 32] where the human operator generates both linear and angular velocity commands $\mathbf{v'_l} := [v_{l_v}, v_{l_\omega}]$ ($\mathbf{v_l} = \mathbf{v'_l}$ when there is no time delay, see Fig. 1), according to the robot position and the goal.
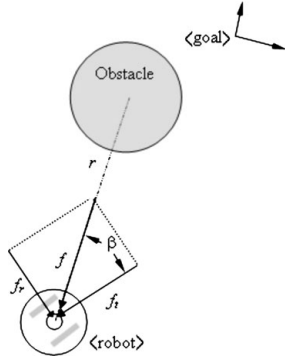
Fig. 4. Fictitious force vector.

The proposed model is the following:

$$\mathbf{v_l'} = \begin{bmatrix} v_{l_v} \\ v_{l_\omega} \end{bmatrix} = \begin{bmatrix} k_v \rho \cos \alpha \\ k_\omega \alpha + k_v \sin \alpha \cos \alpha \end{bmatrix}, \qquad (8)$$

where $k_v, k_\omega > 0$. The parameter k_v depends on how fast the human operator drives the mobile robot according to the distance error ρ, the parameter k_ω establishes mainly the angular velocity generated by the human operator according to the angular error α.

5.2. Fictitious force

To avoid obstacles, it is necessary that the mobile robot interacts with the environment without causing any collision. In such case, the interaction force is represented by a repulsive fictitious force, which depends on the distance between the robot and the obstacle, as shown in Fig. 4.

The magnitude of the repulsive fictitious force f is calculated as

$$f(t) = k_1 - k_2 r(t), \qquad (9)$$

where k_1, k_2 are positive constants such that $k_1 - k_2 r_{\max} = 0$ and $k_1 - k_2 r_{\min} = 1$, $r_{\max}$ is the robot-obstacle maximum distance, $r_{\min}$ is the robot-obstacle minimum distance, and r is the robot-obstacle distance ($r_{\min} \leq r(t) \leq r_{\max}$). The angle of the fictitious force is β which depends on the orientation of the obstacle with respect to the mobile robot (Fig. 4).

The tangential fictitious force and the normal fictitious force are calculated as $f_t = f \cos \beta$ and $f_r = f \sin \beta$, respectively. In this work, only ultrasonic sensors in a frontal range of π rad were used. In the case of using more sensor types, then the fictitious force can be computed from data fusion.[30]

5.3. Models of impedance and decision of the human operator

The impedance model of the human operator is defined as

$$[\rho_e \quad \alpha_e]^T = \mathbf{K}[f_t \quad f_r]^T, \qquad (10)$$

where $\mathbf{K} = \operatorname{diag}[K_\rho \quad K_\alpha]^T$ and $K_\rho, K_\alpha > 0$ describe the human operator's parameters representing his visual impedance, f_t is the fictitious force on the robot motion direction, and f_r is the fictitious force on normal direction to the robot motion direction.

When the mobile robot navigates interacting with the environment, the state is defined as (see Fig. 3)

$$[\tilde{\rho} \quad \tilde{\alpha}]^T = [\rho \quad \alpha]^T - [\rho_e \quad \alpha_e]^T + [\rho_d \quad \alpha_d]^T,$$
$$\text{with} \quad \tilde{\rho} > 0 \quad \text{and} \quad |\tilde{\alpha}| \leq \pi, \qquad (11)$$

where ρ_d, α_d are signals which represent the human operator' decision.

Both, the human's reaction, due to the presence of obstacles on the remote environment, and the human's decision are interpreted as position errors (with respect to the goal) according to the impedance and the internal decision of each human operator.

Remark 1: In general, the parameters k_v, k_ω describing position control and K_ρ, K_α representing visual impedance are different for each human operator and they can be identified.[30]

6. Stability of the nondelayed teleoperation system without decision model

Next, the stability of the nondelayed teleoperation system is analyzed working in free space and considering $\rho_d = 0, \alpha_d = 0$. The goal is to achieve a position reference (without final orientation), this is, that the equilibrium point $[\rho \quad \alpha]^T = 0$ be stable. From (7), the evolution of (ρ, α) is represented by

$$\begin{cases} \dot{\rho} = -v_{l_v} \cos \alpha \\ \dot{\alpha} = -v_{l_\omega} + v_{l_v} \dfrac{\sin \alpha}{\rho} \end{cases}. \qquad (12)$$

When there is no delay, v_{r_v} and v_{r_ω} (velocity of the mobile robot) are similar to v_{lv} and $v_{l\omega}$ (command generated by the human operator), respectively.

From the proposed model of the human operator (8) and the kinematic equations of the mobile robot given by (12), the nondelayed teleoperation system can be described by

$$\begin{cases} \dot{\rho} = -k_v \rho \cos^2 \alpha \\ \dot{\alpha} = -k_\omega \alpha \end{cases}. \qquad (13)$$

Lemma 1.[28] The nondelayed teleoperation system given by (13) (where a mobile robot (12) is driven by a human operator represented by (8)) is exponentially stable with rate $\lambda = \min\{k_v, k_\omega\}$.

7. Control Scheme for Bilateral Teleoperation of a Mobile Robot

The proposed control scheme links a compensation of the time delay based on a human operator's model, a prediction system, and a simple 3D augmented reality scheme. The strategy searches taking advantage of two characteristics: first, the human capability to relate the current robot state with a possible robot state in the near future; and second, the performance of a remote controller (part of the compensation
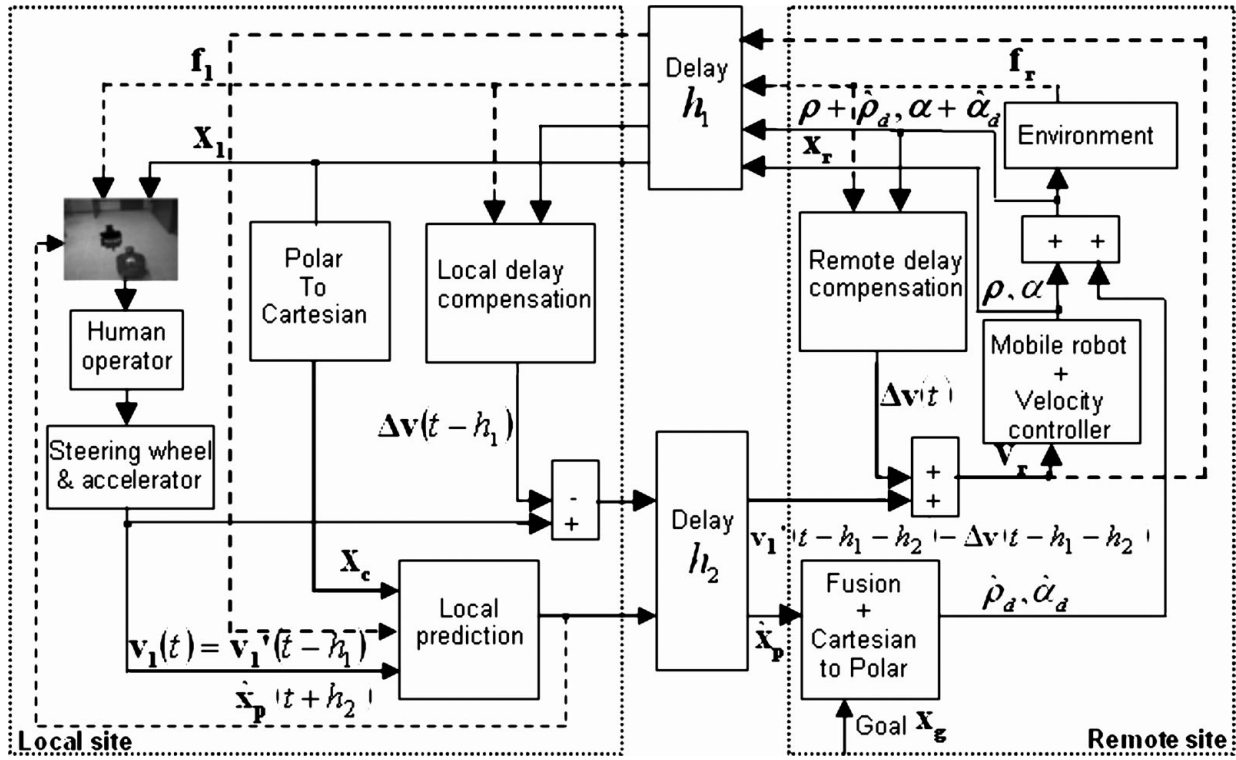
Fig. 5. Proposed control scheme for teleoperation of mobile robots.

of the delay) based on an estimated value of where the human wants to go.

Figure 5 shows a block diagram of the delayed bilateral system introducing the proposed control scheme. Next, we will describe each subsystem of the proposed control scheme.

7.1. Prediction system and its relation with the human operator's decision

The prediction system includes a predictor with bounded output on the local site and a Kalman filter, with a variance that depends on the current fictitious force, on the remote site. The proposed prediction system estimates where the mobile robot will go and where the human operator wants to go in order to help the 3D augmented reality scheme and the delay compensation, respectively; and as a consequence of this, help the human operator.

The proposed prediction algorithm, placed on the local site, estimates where the mobile robot will go $\hat{\mathbf{x}}_\mathbf{p}(t + h_2)$ in h_2 s. The local prediction uses the information that the human operator "sees" ($\mathbf{x}_\mathbf{l}$ and $\mathbf{v}_\mathbf{r}(t - h_1)$), the command $\mathbf{v}_\mathbf{l}$ generated by him and the information about the physical restrictions of both the workspace and the mobile robot, i.e. the maximum linear velocity $v_{\max}$, the maximum angular velocity $\omega_{\max}$, the maximum distance error $\rho_{\max}$ and the maximum angular error $\alpha_{\max}$. Such feedback has a delay of h_1 s with respect to the current time instant.

Then, the output signal of the local predictor $\hat{\mathbf{x}}_\mathbf{p}(t + h_2)$ is sent from the local site to the remote site with a delay of h_2 s. Thus, an estimated position, called $\hat{\mathbf{x}}_\mathbf{p} = [\hat{x}_p \ \hat{y}_p \ \hat{\theta}_p]$, of where the mobile robot will go in the current instant is obtained on the remote site and it is computed as

follows:

$$\hat{\theta}_p(t) = \theta(t - h) + \frac{1}{2}G_\omega[v_{l_\omega}(t - h) + v_{r_\omega}(t - h)]$$

$$\hat{x}_p(t) = x(t - h) + \frac{1}{2}G_v[v_{l_v}(t - h)\cos\hat{\theta}_p(t)$$
$$+ v_{r_v}(t - h)\cos\theta(t - h)]$$

$$\hat{y}_p(t) = y(t - h) + \frac{1}{2}G_v[v_{l_v}(t - h)\sin\hat{\theta}_p(t)$$
$$+ v_{r_v}(t - h)\sin\theta(t - h)]$$

where $G_\omega = \alpha_{\max}/\omega_{\max}\tanh(h/(\alpha_{\max}/\omega_{\max}))$, $G_v = \rho_{\max}/v_{\max}\tanh(h/(\rho_{\max}/v_{\max}))$, $\mathbf{x}_\mathbf{c} = [x \ y \ \theta]$, and v_{r_v}, v_{r_ω} are the position (in Cartesian coordinates) and velocity of the mobile robot, v_{l_v}, v_{l_ω} are the velocity commands (linear and angular, respectively) generated by the human operator, and h (6) is the current time delay (measured in line).

The gains G_v and G_ω assure that the estimated position $\hat{\mathbf{x}}_\mathbf{p}$ is bounded into the workspace of the mobile robot even when h increases to values higher than $\rho_{\max}/v_{\max}$ or $\alpha_{\max}/\omega_{\max}$.

We link the prediction system with the human's model taking the estimated value of where the mobile robot will go in the current instant $\hat{\mathbf{x}}_\mathbf{p}$ as an estimated value of where the human operator wants to go. From this, the human operator's decision represented by ρ_d, α_d can be calculated. We use a decentralized Kalman filter[8] placed on the remote site to fuse the prediction of finite-horizon $\hat{\mathbf{x}}_\mathbf{p}$ with the goal $\mathbf{x}_\mathbf{g}$ in order to estimate $[\hat{\rho}_d \ \hat{\alpha}_d]^T$. Thus, $\mathbf{x}_\mathbf{g}$ is considered in the estimated operator's decision, since it is known and influences the operator's actions. The Kalman filter is implemented in discrete time using a sampling time similar to the ones used in

Fig. 6. Augmented reality overlapping video and a 3D graphics.

the mobile robot (0.1 s in this case). The system is modeled in a standard way as in ref. [5], where the measurement vector is composed by $[\hat{\mathbf{x}}_\mathbf{p} \ \hat{\mathbf{y}}_\mathbf{p} \ \mathbf{x_{g_x}} \ \mathbf{x_{g_y}}]^T$ and the matrix of state transition $\mathbf{A}$ and the observation matrix $\mathbf{H}$ are set to $\mathbf{A} = \mathbf{I}_{2x2}$ and $\mathbf{H} = [\begin{smallmatrix}\mathbf{I}_{2x2}\\\mathbf{I}_{2x2}\end{smallmatrix}]$, with $\mathbf{I}_{2x2}$ the identity matrix. The variance of the Kalman filter is set according to the presence of obstacles. The difference between the estimated state using the Kalman filter and $\mathbf{x_g}$ is converted from Cartesian coordinates to polar coordinates to get $[\hat{\rho}_d \ \hat{\alpha}_d]^T$. The signal $[\rho + \hat{\rho}_d \ \alpha + \hat{\alpha}_d]^T$ represents an estimated subgoal, which is decided by the human operator.

We set the variance of the Kalman filter according to the current tangential fictitious force f_t because when the obstacles are far, the operator's decision mainly depends on the goal position. On the other hand, when the obstacles are near, the operator's decision mainly depends on the current subgoal. Therefore, if the fictitious force increases, then the prediction variance decreases and the goal variance increases.

On the contrary, if the fictitious force decreases, the predictor variance increases and the goal variance decreases. If the fictitious force tends to zero, then $\hat{\rho}_d \to 0$, $\hat{\alpha}_d \to 0$. The behavior of the human operator in this case is mainly described by the impedance and position control models of the human operator.

Note: We remark that the proposed compensation placed on the local and remote sites uses $[\rho + \hat{\rho}_d \ \alpha + \hat{\alpha}_d]^T$ as position reference.

7.2. Augmented reality to the human operator

When there is a large time of uncertainty (large time delay), because the operator does not instantaneously see the corresponding motion of the mobile robot on the local display, the human operator probably generates oscillatory or overshot commands. In order to help the human operator to drive the mobile robot in presence of time delay, video overlapped with a 3D graphic model of a virtual mobile robot is back-feed to the human operator. The camera calibration was included in the graphic engine used (Open GL described in Section 8). Figure 6 shows the information that he/she "sees".

The position and orientation of the virtual mobile robot $\hat{\mathbf{x}}_\mathbf{p}(t + h_2)$ is set from the local predictor, i.e. where the mobile robot will go in h_2 s. Thus, the human operator can decide and apply a command in the current instant based on his/her capability of linking the past and future context.

7.3. Delay compensation

The compensation of the velocity command does not modify the back-fed information (position and fictitious force) from the remote site to the local site. In addition, the local site sends a signal $\mathbf{v_l}(t) - \Delta\mathbf{v}(t - h_1)$ to the remote site; this signal combines the velocity command generated by the human operator $\mathbf{v_l}(t)$ in a time instant t and the compensation $\Delta\mathbf{v}$ calculated from the perceived information (position and force) which stimulates the operator in such moment. In the remote site, the proposed control scheme uses the current position and fictitious force of the remote site to modify the signal $\mathbf{v_l}(t - h_2) - \Delta\mathbf{v}(t - (h_1 + h_2))$ and to establish the velocity reference $\mathbf{v_r}(t)$. The velocity reference $\mathbf{v_r}(t)$ is applied to PID controllers for the linear and angular velocity of the mobile robot.

The control scheme is composed by a compensation of the velocity command placed on both the local and remote sites (Fig. 5) and it is defined by an approximated model of the human operator (8) as follows:

$$\Delta\mathbf{v} = \begin{bmatrix} w_v \\ w_\omega \end{bmatrix} = \begin{bmatrix} \hat{k}_v\tilde{\rho}'\cos\tilde{\alpha}' \\ \hat{k}_\omega\tilde{\alpha}' + \hat{k}_v\sin\tilde{\alpha}'\cos\tilde{\alpha}' \end{bmatrix}, \quad (14)$$

where $\hat{k}_v, \hat{k}_\omega > 0$ are the identified parameters of the human operator,[30] $\Delta\mathbf{v} = [w_v, w_\omega]$ is the output of the proposed delay compensation and

$$[\tilde{\rho}' \ \tilde{\alpha}']^T := [\rho - \hat{K}_\rho f_t + \hat{\rho}_d \ \ \alpha - \hat{K}_\alpha f_r + \hat{\alpha}_d]^T, \quad (15)$$

where $[\hat{\rho}_d \ \hat{\alpha}_d]^T$ is the estimated perturbation signal (which represents the human operator's decision) and

$$\Delta\mathbf{K} = [\Delta K_\rho \ \ \Delta K_\alpha]^T = [K_\rho \ \ K_\alpha]^T - [\hat{K}_\rho \ \ \hat{K}_\alpha]^T \ \text{ and}$$
$$(16)$$
$$[\tilde{\rho}_d \ \ \tilde{\alpha}_d]^T = [\rho_d \ \ \alpha_d]^T - [\hat{\rho}_d \ \ \hat{\alpha}_d]^T \quad (17)$$

represent the parametric error of impedance and the decision model error, respectively. We remark that, unlike our previous papers, the estimated decision of the human operator (given by $\hat{\rho}_d, \hat{\alpha}_d$) is included in the state to control the teleoperation system.

7.4. Stability analysis

Now, we analyze the stability of the teleoperation system incorporating the proposed control scheme. Let us assume that the derivative of the fictitious force is bounded. We will analyze if $\tilde{\rho}$ and $\tilde{\alpha}$, defined in (11), tend to zero.

Considering that the local site is represented by a time-invariant kinematic model, we computed the vector $\mathbf{v_r} = [v_{r_v}, v_{r_\omega}]$ (Fig. 5) as follows:

$$\mathbf{v_r}(t) = \mathbf{v_l}'(t - h) - \Delta\mathbf{v}(t - h) + \Delta\mathbf{v}(t)$$
$$\mathbf{v_r}(t) = \begin{bmatrix} v_{l_v} \\ v_{r_\omega} \end{bmatrix} = \begin{bmatrix} v_{l_v}(t - (h)) - w_v(t - (h)) + w_v(t) \\ v_{l_\omega}(t - (h)) - w_\omega(t - (h)) + w_\omega(t) \end{bmatrix}$$
$$(18)$$

Then, we rewrite (14), using the definitions given by (11), (15)–(17), as follows:

$$
\begin{cases}
w_v = \hat{k}_v \left(\tilde{\rho} + \Delta K_\rho f_t + \tilde{\rho}_d \right) \cos(\tilde{\alpha} + \Delta K_\alpha f_r + \tilde{\alpha}_d) \\
w_\omega = \hat{k}_\omega \left(\tilde{\alpha} + \Delta K_\alpha f_r + \tilde{\alpha}_d \right) \\
\qquad + \hat{k}_v \sin(\tilde{\alpha} + \Delta K_\alpha f_r + \tilde{\alpha}_d) \cos(\tilde{\alpha} + \Delta K_\alpha f_r + \tilde{\alpha}_d)
\end{cases}
$$

$$(19)$$

We assume that $\cos \tilde{\alpha} \approx \cos(\tilde{\alpha} + \Delta K_\alpha f_r + \tilde{\alpha}_d)$ and $\sin \tilde{\alpha} \approx \sin(\tilde{\alpha} + \Delta K_\alpha f_r + \tilde{\alpha}_d)$, i.e. $\Delta K_\alpha f_r + \tilde{\alpha}_d$ is near zero. From (19), the proposed delay compensation can be expressed as

$$
\Delta \mathbf{v} = \begin{bmatrix} w_v \\ w_\omega \end{bmatrix} \approx \begin{bmatrix} \hat{k}_v \left(\tilde{\rho} + \tilde{\rho}_d \right) \cos \tilde{\alpha} + \Delta K_\rho e_{v_z} \\ \hat{k}_\omega \left(\tilde{\alpha} + \tilde{\alpha}_d \right) + \hat{k}_v \sin \tilde{\alpha} \cos \tilde{\alpha} + \Delta K_\alpha e_{\omega_z} \end{bmatrix}
$$

$$(20)$$

where

$$
\begin{aligned}
e_{v_z}(t) &= \hat{k}_v \cos(\tilde{\alpha}) f_t \\
e_{\omega_z}(t) &= \hat{k}_\omega f_r
\end{aligned}
$$

$$(21)$$

are bounded because the tangential fictitious force f_t and the normal fictitious force f_r are bounded signals. The signals $\Delta K_\rho e_{v_z}(t)$, $\Delta K_\alpha e_{\omega_z}(t)$ represent the errors on the estimated velocity generated by errors in the identification of the human operator's impedance.

From (6), (8)—where (ρ, α) are replaced by $(\tilde{\rho}, \tilde{\alpha})$—, and (20), we can write (18) as follows:

$$
\begin{cases}
v_{r_v} = [k_v \tilde{\rho}(t-h) \cos \tilde{\alpha}(t-h)] \\
\qquad - \left[\hat{k}_v \left(\tilde{\rho}(t-h) + \tilde{\rho}_d(t-h) \right) \cos \tilde{\alpha}(t-h) \right] \\
\qquad + \left[\hat{k}_v \left(\tilde{\rho}(t) + \tilde{\rho}_d(t) \right) \cos \tilde{\alpha}(t) \right] + \Delta K_\rho \Delta e_{v_z}(\cdot) \\
v_{r_\omega} = [k_\omega \tilde{\alpha}(t-h) + k_v \sin \tilde{\alpha}(t-h) \cos \tilde{\alpha}(t-h)] \\
\qquad - [\hat{k}_\omega(\tilde{\alpha}(t-h) + \tilde{\alpha}_d(t-h)) + \hat{k}_v \sin \tilde{\alpha}(t-h) \cos \tilde{\alpha}(t-h)] \\
\qquad + [\hat{k}_\omega(\tilde{\alpha}(t) + \tilde{\alpha}_d(t)) + \hat{k}_v \sin \tilde{\alpha}(t) \cos \tilde{\alpha}(t)] + \Delta K_\alpha \Delta e_{\omega_z}(\cdot)
\end{cases}
$$

$$(22)$$

where the signals $\Delta e_{v_z}(.) = e_{v_z}(t) - e_{v_z}(t-h)$ and $\Delta e_{\omega_z}(.) = e_{\omega_z}(t) - e_{\omega_z}(t-h)$ are bounded.

From the kinematic equations of a mobile robot detailed in ref. [1] and considering the time-varying goal (due to the presence of fictitious force), the evolution of the state $[\tilde{\rho} \ \tilde{\alpha}]^T$ of the teleoperation system can be described by

$$
\begin{cases}
\dot{\tilde{\rho}} = -v_{r_v} \cos \tilde{\alpha} + K_\rho \dot{f}_t + \dot{\rho}_d \\
\dot{\tilde{\alpha}} = -v_{r_\omega} + v_{r_v} \dfrac{\sin \tilde{\alpha}}{\tilde{\rho}} - \dfrac{(K_\alpha \dot{f}_r + \dot{\alpha}_d)}{\tilde{\rho}}
\end{cases}
$$

$$(23)$$

The teleoperation system described by (23) has a singularity when $\tilde{\rho} = 0$. We add a perturbation $v_{p'}$ to the linear velocity v_{r_v} of the mobile robot avoiding $\tilde{\rho}$ near zero, including when no obstacles exist on the path of the mobile robot. Then, we define $v_{p'}$ as

$$
\begin{aligned}
&\text{IF } \tilde{\rho} < \eta = \text{TRUE} \\
&v_{p'} = -K_w \left(|f_t + f_g| + \varepsilon \right) \cos \tilde{\alpha} < 0 \qquad (24) \\
&\text{ELSE} \qquad v_{p'} = 0,
\end{aligned}
$$

where $K_w > 0$, $\varepsilon > 0$, η is a positive constant which indirectly defines the value of $\tilde{\rho}$ smaller than the compensated singularity, f_t is the repulsive tangential fictitious force, and f_g is a repulsive fictitious force from a virtual obstacle placed on the goal.

Finally, we incorporate (22) and (24) into (23) representing the delayed teleoperation system as follows:

$$
\begin{bmatrix} \dot{\tilde{\rho}} \\ \dot{\tilde{\alpha}} \end{bmatrix} = f_1(\tilde{\rho}, \tilde{\alpha}) + g_1(\tilde{\rho}, \tilde{\alpha}, \tilde{\rho}(t-h), \tilde{\alpha}(t-h), \dot{\rho}_d, \dot{\alpha}_d, \dot{f}_t, \dot{f}_r)
$$

$$(25)$$

where

$$
\begin{aligned}
f_1(\tilde{\rho}, \tilde{\alpha}) &= \begin{bmatrix} -\hat{k}_v \tilde{\rho} \cos^2 \tilde{\alpha} \\ -\hat{k}_\omega \tilde{\alpha} \end{bmatrix} \\
g_1(\tilde{\rho}, \tilde{\alpha}, \tilde{\rho}(t-h), \tilde{\alpha}(t-h)) &= g_{1a}(.) + g_{1b}(.) + g_{1c}(.) + g_{1d}(.)
\end{aligned}
$$

with

$$
g_{1a}(.) = \begin{bmatrix} -\tilde{k}_v \tilde{\rho}(t-h) \cos \tilde{\alpha}(t-h) \cos \tilde{\alpha} \\ -\tilde{k}_\omega \tilde{\alpha}(t-h) + \tilde{k}_v \tilde{\rho}(t-h) \cos \tilde{\alpha}(t-h) \\ \times \left(\dfrac{\sin \tilde{\alpha}}{\tilde{\rho}} - \dfrac{\sin \tilde{\alpha}(t-h)}{\tilde{\rho}(t-h)} \right) \end{bmatrix}
$$

$$
g_{1b}(.) = \begin{bmatrix} -\Delta K_\rho \cos \tilde{\alpha} \Delta e_{v_z}(t, t-h) \\ -\Delta K_\alpha \Delta e_{\omega_z}(t, t-h) + \Delta K_\rho \dfrac{\sin \tilde{\alpha}}{\tilde{\rho}} \Delta e_{v_z}(t, t-h) \end{bmatrix}
$$

$$
g_{1c}(.) = \begin{bmatrix} -\hat{k}_v \cos \tilde{\alpha}(\tilde{\rho}_d \cos \tilde{\alpha} - \tilde{\rho}_d(t-h) \cos \tilde{\alpha}(t-h)) \\ -\hat{k}_\omega(\tilde{\alpha}_d - \tilde{\alpha}_d(t-h)) - \hat{k}_v \dfrac{\sin \tilde{\alpha}}{\tilde{\rho}}(\tilde{\rho}_d \cos \tilde{\alpha} \\ \quad - \tilde{\rho}_d(t-h) \cos \tilde{\alpha}(t-h)) \end{bmatrix}
$$

$$
g_{1d}(.) = \begin{bmatrix} K_\rho \dot{f}_t + \dot{\rho}_d - v_{p'} \cos \tilde{\alpha} \\ -\dfrac{K_\alpha \dot{f}_r + \dot{\alpha}_d}{\tilde{\rho}} + v_{p'} \dfrac{\sin \tilde{\alpha}}{\tilde{\rho}} \end{bmatrix}
$$

Now, we define a new variable as $\tilde{\rho}_m = \tilde{\rho} - \eta$ with $\eta(t) = (K_w/\hat{k}_v)(|f_t + f_g| + \varepsilon) > 0$ for all t, to make a variable changing in (25) replacing $\tilde{\rho}$ for $\tilde{\rho} = \tilde{\rho}_m + \eta$. We remark that $\tilde{\rho}_m + \eta > 0$ for all t. From this, (25) can be rewritten as (4) plus a perturbation signal of the following way:

$$
\begin{bmatrix} \dot{\tilde{\rho}}_m \\ \dot{\tilde{\alpha}} \end{bmatrix} = f_1(\tilde{\rho}_m, \tilde{\alpha}) + g_1(\tilde{\rho}_m, \tilde{\alpha}, \tilde{\rho}_m(t-h), \tilde{\alpha}(t-h)) + p(.),
$$

$$(26)$$

where

$$
f_1(\tilde{\rho}_m, \tilde{\alpha}) = \begin{bmatrix} -\hat{k}_v \tilde{\rho}_m \cos^2 \tilde{\alpha} \\ -\hat{k}_\omega \tilde{\alpha} \end{bmatrix}
$$

represents the nondelayed teleperation system;

$$g_1\left(\tilde{\rho}_m, \tilde{\alpha}, \tilde{\rho}_m(t-h), \tilde{\alpha}(t-h)\right)$$

$$= \begin{bmatrix} -\tilde{k}_v \tilde{\rho}_m(t-h)\cos\tilde{\alpha}(t-h)\cos\tilde{\alpha} \\ -\tilde{k}_\omega \tilde{\alpha}(t-h) + \tilde{k}_v\left(\tilde{\rho}_m(t-h)+\eta\right)\cos\tilde{\alpha}(t-h) \\ \times \left(\dfrac{\sin\tilde{\alpha}}{\tilde{\rho}_m+\eta} - \dfrac{\sin\tilde{\alpha}(t-h)}{\tilde{\rho}_m(t-h)+\eta}\right) \end{bmatrix}$$

represents the delayed dynamics of the teleoperation system, and

$$p\left(\tilde{\rho}, \dot{\rho}_d, \dot{\alpha}_d, \dot{f}_t, \dot{f}_r\right) = p_1 + p_2 + p_3 + p_4$$

is a perturbation signal, where

$$p_1(.) = \begin{bmatrix} (-\tilde{k}_v \cos\tilde{\alpha}(t-h)\cos\tilde{\alpha} + \hat{k}_v \cos^2\tilde{\alpha})\eta(t) \\ \hat{k}_v \cos\tilde{\alpha}\sin\tilde{\alpha}\dfrac{1}{\tilde{\rho}_m+\beta(t)}\eta(t) \end{bmatrix}$$

depends on the signal $\eta(t)$ added by the proposed scheme to avoid the system singularity,

$$p_2(.) = \begin{bmatrix} -\cos\tilde{\alpha}\Delta K_\rho \Delta e_{v_z}(t, t-h) \\ -\Delta K_\alpha \Delta e_{\omega_z}(t, t-h) \\ +\Delta K_\rho \dfrac{\sin\tilde{\alpha}}{\tilde{\rho}_m+\eta}\Delta e_{v_z}(t, t-h) \end{bmatrix}$$

depends on the parametric errors of the human operator's estimated impedance,

$$p_3(.) = \begin{bmatrix} -\hat{k}_v \cos\tilde{\alpha}\left(\tilde{\rho}_d \cos\tilde{\alpha} - \tilde{\rho}_d(t-h)\cos\tilde{\alpha}(t-h)\right) \\ -\hat{k}_\omega\left(\tilde{\alpha}_d - \tilde{\alpha}_d(t-h)\right) - \hat{k}_v\dfrac{\sin\tilde{\alpha}}{\tilde{\rho}_m+\eta(t)} \\ \times\left(\tilde{\rho}_d \cos\tilde{\alpha} - \tilde{\rho}_d(t-h)\cos\tilde{\alpha}(t-h)\right) \end{bmatrix}$$

depends on the estimation errors of the human operator's decision, and

$$p_4(.) = \begin{bmatrix} K_\rho \dot{f}_t + \dot{\rho}_d \\ -\dfrac{K_\alpha \dot{f}_r + \dot{\alpha}_d}{\tilde{\rho}_m+\eta(t)} \end{bmatrix}$$

depends on the derivative of the fictitious force and the derivative of the human operator's decision.

Note: In (25) and (26), the dependence of t has not been pointed to simplify the notation.

We assume the parametric errors (given by $[\tilde{k}_v, \tilde{k}_\omega]$ and $[\Delta K_\rho, \Delta K_\alpha]$) and the errors $[\tilde{\rho}_d, \tilde{\alpha}_d]$ bounded, then $|g_1|$ in (26) will also be bounded. We termed the delayed teleoperation system described by (26) without perturbation ($p(\cdot) = 0$) as the nominal system.

From Fact 2 and Lemma 1 apply to the nominal system, we can establish that the equilibrium point $[\rho_m \ \rho_m(t-h) \ \alpha \ \alpha(t-h)] = \mathbf{0}$ is exponentially stable if

$$|g_1| < \min\{\hat{k}_v, \hat{k}_\omega\}\frac{1-\tau}{2-1.5\tau}. \tag{27}$$

Equation (27) establishes a bound for the errors of the human operator's model depending on the exponential stability of the nondelayed teleoperation system and the maximum derivative τ of the time delay h.

If the nominal system verifies condition (27), it can be represented by a stable exponentially nondelayed system with coefficients c_1, c_2, c_3, c_4, defined in ref. [15, p. 204], given from Corollary 1 by

$$\begin{aligned} c_1 &= a = \frac{1}{2} \\ c_2 &= b \\ c_3 &= \frac{c}{d^2} \\ c_4 &= 1 \end{aligned} \tag{28}$$

In addition, if the perturbation is bounded $p(\cdot) \le \delta$ for all $t \ge 0$ and for all $[\rho_m \ \rho_m(t-h) \ \alpha \ \alpha(t-h)]$, then we can apply Lemma 5.2 of ref. [15, p. 213] to (26) considering (28), establishing that the delayed teleoperation system adding the proposed control scheme will be ultimately bounded to a ball of size B given by

$$B = \sqrt{2}\frac{\delta}{\theta}\frac{\sqrt{b}}{b}\frac{b}{c}d^2 < \sqrt{2}\frac{\delta}{\theta}\frac{b}{c}d^2, \tag{29}$$

with an exponential decreasing rate γ given by

$$\gamma = \frac{(1-\theta)}{2}\frac{c}{b}\frac{1}{d^2}, \tag{30}$$

where $0 < \theta < 1$ is a positive arbitrary constant which shows a trade-off between a faster decreasing rate and a smaller convergence ball. From Fact 1, the higher the time delay, the higher the d is, making the convergence ball (29) greater and the decreasing rate (30) lower.

The proposed control scheme is based on a model of the human operator. If the errors of such model are smaller, then $|g_1|$ also decreases, and from Corollary 1, the relation c/b increases. But, from Fact 1, d depends on c/b. Then, if c/b ensures that d meets Corollary 2 for a given time delay, then the convergence ball (29) will be smaller and the decreasing rate (30) will be higher. Although the nominal system meets exponential stability (27) independently from the maximum time delay, the real system (perturbed teleoperation system) will have a practical bound for the time delay (since c/b cannot infinitely be increased as the errors of the human operator's model tend to zero) where the system will work well, error B (29) and the decreasing rate γ (30) according to the requirements of a given application.

Remark 2: The proposed control scheme assures the convergence to zero of $\tilde{\rho}$ and $\tilde{\alpha}$. This does not guarantee that the mobile robot achieves the goal ($[\rho \ \alpha]^T = \mathbf{0}$), as for example, the case of multi-obstacles obstructing the path between the robot and the goal. However, $\tilde{\rho}$ and $\tilde{\alpha}$ include the human operator's decision so he/she can change his/her decision to avoid unwanted static positions of the mobile robot.
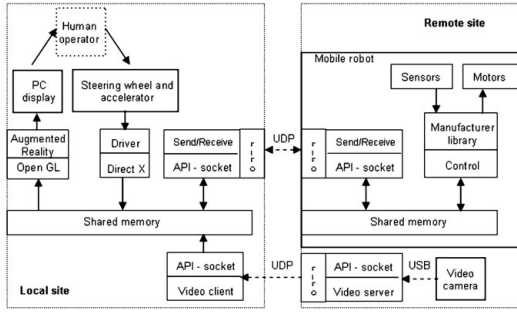
Fig. 7. Software structure developed to implement the proposed control scheme.

Fig. 8. Trajectories of the mobile robot teleoperated for different delays.

8. Control Scheme for Bilateral Teleoperation of a Mobile Robot

The software developed for robots teleoperation is based on multi-process and multi-threads running under Windows platforms. Visual C++, API Windows, Open GL, Direct X, and the robot manufacturer libraries were used to build our applications. The software structure is composed by various processes running on two or three PCs (including the PC on board of the mobile robot); one or two PCs are placed on the remote site and the other one is placed on the local site. Figure 7 shows a block diagram of the developed software system.

The processes running on each PC share data through shared memory and the control and video data are sent via IP/UDP protocol using different sockets. The video source can be the robot video camera or an external camera (in this work, a webcam is used). The PC placed on the local site and the mobile robot are linked via Wireless Intranet using the IP/UDP protocol The time delay is simulated through FIFO buffers (time-varying length) placed both on the local and remote sites. On the other hand, a process-based Direct X library links the PC and the steering wheel via USB port.

The human operator receives the image provided by a video camera placed on the remote site overlapped with a 3D graphic model of the mobile robot. This graphic model was designed using Open GL. In such model, the physical dimensions of the real mobile robot are considered as well as the view point of the used webcam including its intrinsic parameters.

We remark that another mobile robot could be used only by replacing the library provided by the robot's manufacturer.

9. Experiments

The control objective is that a mobile robot, driven by a human operator at distance, achieves an established goal avoiding a cube-type obstacle placed opposite the mobile robot.

We use a Pioneer 2DX mobile robot (www.activmedia. com). In addition, the human operator perceives delayed visual feedback from a remote webcam and generates the velocity commands through a steering wheel and accelerator pedal. The local site and the remote site are two laboratories at San Juan University, in Argentina; and they are linked via Intranet using the IP/UDP protocol. In this case, the delay
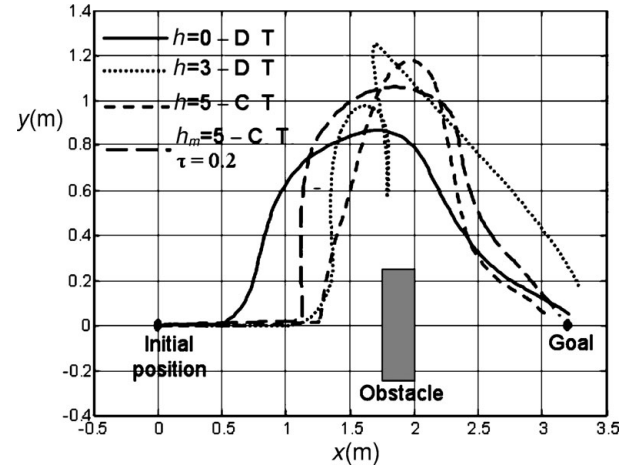
added by the Intranet is very small, so we increase it using FIFO buffers of a controlled size.

The initial condition is $\rho(\theta) = 3.2$ m, $\alpha(\theta) = 0$ rad for $\theta \in [-h(t_0), 0]$. We set the parameter $K_w = 0.5$ m/Ns to compensate the singularity in $\tilde{\rho} = 0$. The parameters of the PID velocity controller (on board of the mobile robot) are $K_p = 30$ (proportional gain), $K_d = 60$ (derivative gain), and $K_i = 2$ (integral gain) for the linear and angular velocity control of the mobile robot. The mobile robot sends sensorial information and receives velocity references from the control computer every 0.1 s, but the PID controller of each electrical engine run faster so the velocity reference is achieved in few sample periods. We remark that the information on the units of the PID parameters and the sampling time of the closed loop control of the motors are not documented by the robot's manufacturer. On the other hand, the fictitious force is computed when the mobile robot detects an obstacle at a distance less than 1.5 m using the frontal ultrasonic sensors.

The parameters used by the proposed control scheme to represent the human operator are similar to the ones used in refs. [30, 31], where they were identified using the gradient method and the RLS algorithm), that is

$$\hat{k}_v = 0.45 \text{ m/s}, \hat{k}_\omega = 0.45 \text{ rad/s},$$
$$\hat{K}_\rho = 5 \text{ m/N}, \hat{K}_\alpha = 1.5 \text{ rad/s}.$$

Figure 8 shows the trajectories executed by the mobile robot driven by a human operator with direct teleoperation (DT) and compensated teleoperation (CT) for different time delays (see Fig. 9) generated from FIFO buffers. We remark that when the human operators drive the mobile robot, they do not know the delay.

Using the proposed control scheme, the mobile robot (driven by the human operator) avoids the obstacle with a "soft" trajectory in presence of both constant time delay and time-varying delay.

Figure 10 shows the evolution of the normal and tangential fictitious forces. The smaller the obstacle-robot distance, the greater the fictitious force is.
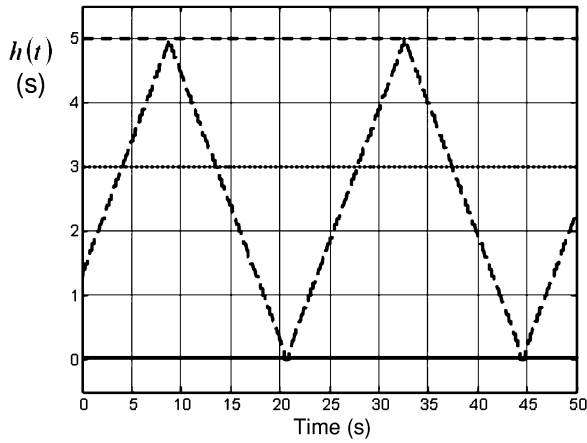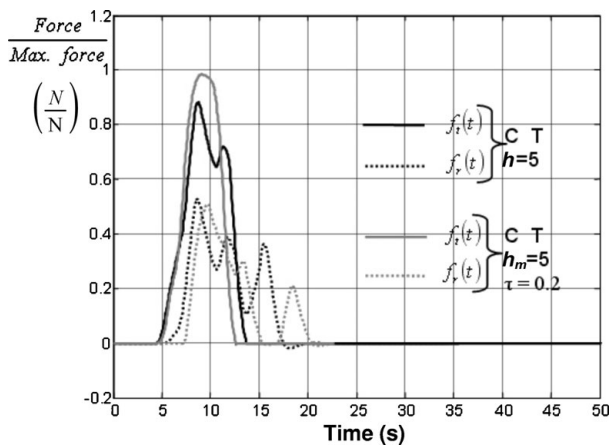
Fig. 9. Time delay for the experiments.

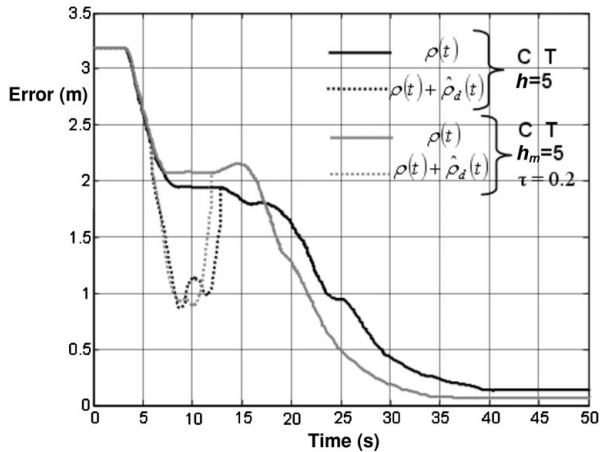Fig. 10. Normal and tangential fictitious force.

Fig. 11. Temporal evolution of both the distance error ρ and $\rho + \hat{\rho}_d$.

Fig. 12. Temporal evolution of the angular error α and $\hat{\alpha}_d$.

Fig. 13. Linear velocity command generated by the human operator and compensated linear velocity reference.

Figure 11 shows the evolution of both the distance error ρ and the error $\rho + \hat{\rho}_d$ which is calculated from the mobile robot position and the estimated subgoal. Using the proposed control scheme, the distance error tends to a lower bound in a finite time.

Figure 12 shows the evolution of the angular error α (main plot) and the estimated decision $\hat{\alpha}_d$ (subplot on the bottom right corner). The estimated decision $\hat{\alpha}_d$ appears when the human operator decides whether to turn left or right in presence of the obstacle.
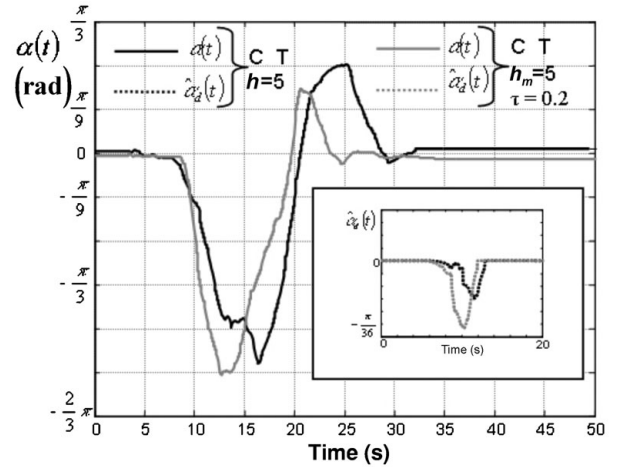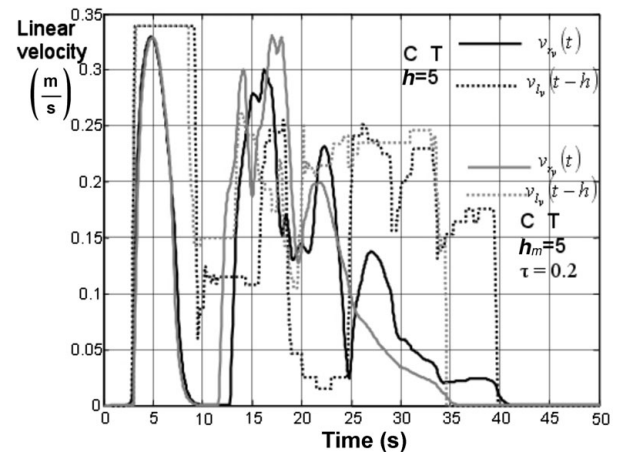
We remark that when an obstacle appears (5 s of the experiment approximately) the remote impedance of the delay compensation makes the mobile robot velocity decrease. Then, the position controller of the delay compensation uses the estimated subgoal, provided by the prediction system, to help the human operator "go" in a desired direction, avoiding a collision in spite of large time delay. Figures 13 and 14 show the linear and angular velocity commands (on the remote site) sent by the human operator from the local site, and the linear and angular velocity references compensated by the proposed control scheme for constant delay and time-varying delay.

The proposed control scheme pushes the velocity references to more conservative values in presence of obstacles and time delay, avoiding collisions.

Table I summarizes the obtained results based on 10 experiments for different conditions of teleoperation.

The experiments results on the teleoperation of a mobile robot with visual feedback have shown a stable behavior and a good performance using the proposed control scheme in presence of obstacles and both constant time delay and time-varying delay.

Table I. Summary of teleoperation experiments.

Teleoperation	h_m (s), r	Average time to the goal (s)	Collision 1 obstacle (%)
DT	0, 0	14.4	0
DT	3, 0	60	50
DT	5, 0	×	100
CT	5, 0	23	0
CT	5, 0.4	22	0

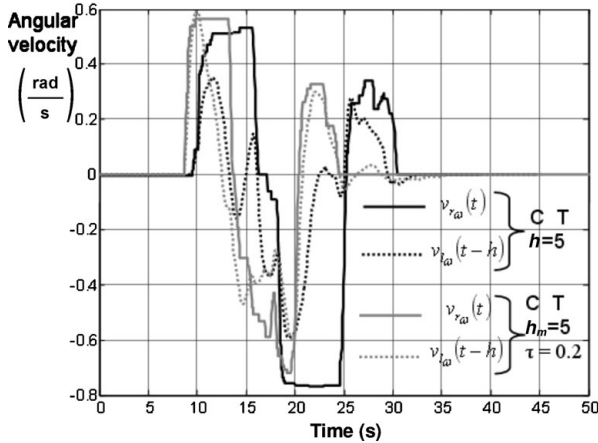x: The time average is not computed due to the mobile robot never achieves the goal

Fig. 14. Angular velocity command generated by the human operator and compensated angular velocity reference.

10. Conclusions

The design of control schemes for robots teleoperation requires taking advantage of the human operator's capability. The proposed scheme links a compensation of the time delay based on a human's model, a 3D augmented reality scheme and a prediction system. This strategy searches taking advantage of the human's capabilities to integrate past information from the delayed video with future information from a 3D graphics based on prediction, and decide an "intelligent" action in the current instant. This command generated by the human operator has an important part related with the human's decision which is prioritized by the bilateral compensation scheme since it compensates the delayed human's reaction without changing the decision, based on visual feedback (augmented reality), taken by him.

The control scheme has a fast response in presence of obstacles because it acts in the remote site making use of the impedance and the position controller included into the delay compensation. In addition, such remote position controller "pushes" the mobile robot to "the place the human wants to go."

The designed teleoperation system is ultimately bounded with an exponential decreasing rate. The stability analysis made in this paper proves that the higher the time delay, the greater and the lower the convergence ball and the decreasing rate are.

Several experiments on teleoperation, using the proposed control scheme, have shown a stable response in presence of a maximum time delay about 5 s. This bound is bigger than those achieved in our previous papers.

As future work, we will make experiments in outdoor navigation scenarios, where the video camera will be placed on board the mobile robot considering the final goal, unknown as well as complex environments including different static and mobile objects and people in order to obtain a measure about to what extent the proposed control scheme could be applied.

References
1. M. Aicardi, G. Casalino, A. Bicchi and A. Balestrino, "Closed loop steering of unicycle-like vehicles via Lyapunov techniques," *IEEE Rob. Automat. Mag.* **2**, 27–35 (1995).
2. R. J. Anderson and M. Spong, "Bilateral control of teleoperators with time delay," *IEEE Trans. Automat. Control* **34**(5), 494–501 (1989).
3. P. Arcara and C. Melchiorri, "Control schemes for teloperation with time delay: A comparative study," *Rob. Autonom. Syst.* **38**, 49–64 (2002).
4. A. K. Bejczy, W. S. Kim and S. C. Venema, "The Phantom Robot: Predictive Displays for Teleoperation with Time Delay," *Proceedings of the IEEE International Conference on Robotics and Automation*, Cincinnati, OH (1990) pp. 546–551.
5. G. Bishop and G. Welch, *An Introduction to the Kalman Filter,* Course 8 Presented at ACM SIGGRAPH (University of North Carolina, Chapel Hill, 2001).
6. K. Brady and T. J. Tarn, "Internet-Based Teleoperation," *Proceedings of the 2000 IEEE International Conference on Robotics & Automation*, Seoul, Korea (2000) pp. 843–848.
7. T. A. Burton, "Stability and Periodic Solutions of Ordinary and Functional Differential Equations," **In**: *Mathematics in Science and Engineering,* vol. 178 (Academic Press, New York, 1985).
8. R. Brown and P. Hwang, *Introduction to Random Signals and Applied Kalman Filtering*, 3rd ed. (John Wiley & Sons, New York, 1997).
9. N. Chopra and M. W. Spong, "Bilateral Teleoperation over the Internet: the Time Varying Delay Problem," *Proceedings of the American Control Conference,* Denver, Colorado (Jun. 4–6, 2003), pp. 155–160.
10. R. D. Driver, "Existence and stability of solutions of a delay-differential system," *Arch. Rational Mech. Anal.* **10**, 401–426 (1962).
11. I. Elhajj, N. Xi, W. K. Fung, Y. H. Liu, Y. Hasegawa and T. Fukuda, "Supermedia-enhanced internet-based telerobotics," *Proc. IEEE* **91**(3), 396–421 (2003).
12. J. Funda and R. P. Paul, "Teleprogramming: Toward delay-invariant remote manipulation," *Presence: Teleoperators Virtual Environ.* **1**(1), 29–44 (1992).
13. M. Hernando and E. Gambao, "A Robot Teleprogramming Architecture," *Proceedings of the International Conference on Advanced Intelligent Mechatronics*, Port Island, Kobe, Japan (2003) pp. 1113–1118.
14. P. F. Hokayem and M. W. Spong, "Bilateral teleoperation: An historical survey," *Automatica* **42**, 2035–2057 (Dec. 2006).
15. H. K. Khalil, *Nonlinear Systems*, 2nd ed. (Prentice Hall, New York, 1996). Editorial, ISBN 0–13-228024–8.
16. J. Kikuchi, K. Takeo and K. Kosuge, "Teleoperation System via Computer Network for Dynamic Environment," *Proceedings of the 1998 IEEE International Conference on Robotics and Automation*, Leuven, Belgium (1998) pp. 3534–3539.

17. W. Kim, B. Hannaford and A. Bejczy, "Force reflection and shared compliant control in operating telemanipulators with time delay," *IEEE Trans. Rob. Automat.* **8**(2), 76–185 (1992).

18. D. A. Lawrence, "Stability and transparency in bilateral teleoperation," *IEEE Trans. Rob. Automat.* **9**(5) 624–637 (1993).

19. S. Leeraphan, T. Maneewan and S. Laowattana, "Stable Adaptive Bilateral Control of Transparent Teleoperation through Time-Varying Delay," *Proceeding of the International Conference on Intelligent Robots and Systems (IROS 2002)*, Lausanne, Switzerland (Sep. 30–Oct. 4, 2002).

20. S. Munir and W. J. Book, "Internet-based teleoperation using wave variables with prediction," *IEEE/ASME Trans. Mechatron.* **7**(2), 124–133 (2002).

21. S. I. Niculescu, *Delay Effects on Stability* (Springer Verlag, New York, 2001).

22. G. Niemeyer and J. J. E. Slotine, "Stable adaptive teleoperation," *IEEE J. Oceanic Eng.* **16**(1), 152–162 (1991).

23. J. H. Park and H. C. Cho, "Sliding-mode Control of Bilateral Teleoperation Systems with Force-Reflection on the Internet," *Proceedings of IEEE/RSJ International Conference on Intelligent Robots and Systems*, Takamatsu, Japan (2000) pp. 1187–1192.

24. J. P. Richard, "Time-delay systems: an overview of some recent advances and open problems," *Automatica* **39**, 1667–1694 (2003).

25. J. Sheng and M. Spong, "Model Predictive Control for Bilateral Teleoperation Systems with Time Delays," *Proceedings of IEEE CCECE '04 – CCGEI '04*, Niagara Falls (2004) pp. 1877–1880.

26. T. B. Sheridan, *Telerobotics, Automation, and Human Supervisory Control* (The MIT Press, Cambridge, MA, 1992).

27. T. B. Sheridan, "Teleoperation, telerobotics and telepresence: A progress report," *Control Eng. Pract.* **3**(2), 205–214 (1995).

28. E. Slawiñski, V. Mut and J. F. Postigo, "Bilateral Teleoperation of Mobile Robots with Delay," *Proceedings of the IEEE ICMA05*, Niagara Falls, Canada (2005) pp. 1672–1677.

29. E. Slawiñski, V. Mut and J.F. Postigo, "Stability of systems with time-varying delay," *Latin Am. Appl. Res.* (LAAR), **36**(1), 41–48 (2006).

30. E. Slawiñski, J. Postigo, V. Mut and C. Soria, "Bilateral Teleoperation of Mobile Robots through Internet," *Proceeding of the 8th International IFAC Symposium on Robot Control SYROCO 2006*, Bologna, Italy (2006).

31. E. Slawiñski, J. Postigo and V. Mut, "Stable Teleoperation of Mobile Robots," *Proceeding of the IEEE ICMA 2006*, China (2006) pp. 318–323.

32. E. Slawiñski, V. Mut and J. Postigo, "Teleoperation of mobile robots with time-varying delay," *Robotica* **55**, 205–215 (2006).

33. E. Slawiñski, J. Postigo and V. Mut, "Bilateral teleoperation through the internet," *Rob. autonom. Syst.* **55**, 205–215 (2007).

34. S. Stramigioli, C. Secchi, A. J. van der Schaft and C. Fantuzzi, "Sampled data systems passivity and discrete port-Hamiltonian systems," *IEEE Trans. Rob.* **21**(4), 574–587 (2005).

35. J. Ueda and T. Yoshikawa, "Force-reflecting bilateral teleoperation with time delay by signal filtering," *IEEE Trans. Rob. Automat.* **20**(3), 613–619 (2004).

36. Y. Yokokohji, T. Tsujioka and T. Yoshikawa, "Bilateral Control with Time-Varying Delay including Communication Blackout," *Proceedings of the 10th Symposium on Haptic Interfaces for Virtual Environment and Teleoperator Systems*, Orlando, USA (2002) pp. 285–292.

37. C. Zhang, Y. Lee and K. T. Chong, "Passive Teleoperation Control with Varying Time Delay," *Proceedings of the 9th IEEE International Workshop on Advanced Motion Control*, Istanbul, Turkey (2006) pp. 23–28.